Developmental Biology **247,** 116–126 (2002)
doi:10.1006/dbio.2002.0678

in the Regulation of Heart Development

Wendy V. Gerber,[1,2] Steven A. Vokes,[1] N. Ruth Zearfoss,[3] and Paul A. Krieg[4]

Department of Cell Biology and Anatomy, University of Arizona Health Sciences Center, 1501 N. Campbell Avenue, P.O. Box 245044, Tucson, Arizona 85724

RNA-binding proteins are known to play an important role in a number of aspects of development, although in most cases the precise mechanism of action remains unknown. We have previously described the isolation of an RNA-binding protein, hermes, that is expressed at very high levels in the differentiating myocardium. Here, we report experiments aimed at elucidating the functional role of hermes in development. Utilizing the *Xenopus* oocyte, we show that hermes is localized primarily to the cytoplasm, can associate in a multiprotein complex, and is able to bind to mature RNA transcripts *in vivo*. Overexpression of hermes in the developing embryo dramatically and specifically inhibits heart development. In particular, transcripts encoding the myocardial differentiation markers, *cardiac troponin I* and *cardiac α-actin*, are absent, and overall morphological development of the heart is eliminated. Examination of markers of precardiac tissue showed that expression of *GATA-4* is normal, while the levels of *Nkx2–5* mRNA are strongly reduced. Overall, these studies suggest that hermes plays a role in the regulation of mature transcripts required for myocardial differentiation. To our knowledge, this is the first evidence for an RNA-binding protein playing a direct role in regulation of vertebrate heart development.

Key Words: **RNP domain; Nkx2–5; GATA-4; cardiac development; kidney development; morpholino oligonucleotides.**

INTRODUCTION

The majority of molecular studies of early heart development have focused on the identification and characterization of growth factors and transcription factors expressed in the cardiogenic region and in the heart. At the very earliest stages of heart development, BMP signaling and localized inhibition of Wnt signaling are required for a subset of mesodermal cells to become specified to a cardiac fate (reviewed in Olson, 2001). Coincident with these early signaling events, transcription factors crucial for cardiac specification and differentiation are expressed. These include members of the tinman, GATA, MEF2, and Hand gene families (reviewed in Bodmer and Venkatesh, 1998; Evans, 1999; Harvey *et al.*, 1999).

Given the complex series of events involved in organogenesis and cellular differentiation, it seems likely that posttranscriptional mechanisms will also be employed to fine tune the broader programs regulated by growth and transcription factors. Indeed, a body of evidence indicates that numerous different developmental processes are regulated at the level of RNA splicing, stability, localization, or translation. One of the best characterized examples occurs during axis formation in *Drosophila*, where localization of specific RNA transcripts and translational regulation of their expression is essential for correct A/P axis formation (Grunert and St. Johnson, 1996; Curtis, 1994). Furthermore, differentiation of neurons in the *Drosophila* embryo is dependent on the correct splicing and translation of messages, mediated by the RNA-binding protein, elav (Koushika *et al.*, 1996; Antic and Keene, 1997; Antic *et al.*, 1999; Perron *et al.*, 1999). Although they are not generally as well characterized, a number of RNA-binding proteins are also known to be involved in vertebrate development. For example, DAZ and SpnR are required during mammalian sperm development (Hauberman *et al.*, 1998; Schumacher *et al.*, 1998), Quaking is essential for myelinization of central nervous system neurons in the mouse (Ebersole *et al.*, 1996) and for notochord formation in *Xenopus* (Zorn

[1] These authors contributed equally to this work.
[2] Present address: Max-Planck-Institut für biophysikalische Chemie, Abt. Molekulare Entwicklungsbiologie, Am Fassberg 11, D-37077 Göttingen, Germany.
[3] Present address: Department of Molecular Genetics, University of Texas MD Anderson Cancer Center, 1515 Holcombe Drive, Houston, TX 77030.
[4] To whom correspondence should be addressed. Fax: (520) 626-2097. E-mail: pkrieg@email.arizona.edu.

0012-1606/02 $35.00

and Krieg, 1997), and hnRNP-H plays a role during visceral myogenesis (Liu *et al.*, 2001). In addition, defects in expression of the FMR1 protein are responsible for fragile-X syndrome in humans (Kaufmann and Reiss, 1999)

Based on the presence of recognizable sequence motifs, hundreds of other RNA-binding proteins have been identified in vertebrates. While their precise functions remain largely unknown, it is likely that a large proportion are involved in posttranscriptional regulation of gene expression. One of the largest and best-characterized families of RNA-binding proteins is the RNA Recognition Motif (RRM) family. Members of the RRM family contain one or more copies of a structurally conserved 80- to 100-amino-acid domain, which includes two regions of 6–8 highly conserved residues called RNP1 and RNP2. The RNP1 and RNP2 domains are involved with direct contact of RNA and are required for RNA binding (Nagai *et al.*, 1990; Hoffman *et al.*, 1991). RRM proteins appear to be involved in all aspects of RNA metabolism and are thought to mediate their interactions through sequence-specific rather than promiscuous binding to RNA (Burd and Dreyfuss, 1994). RRM family sequences with a known developmental role include *sex lethal* (Bell *et al.*, 1988), *elav* (Robinow *et al.*, 1988), and *squid* (Kelley *et al.*, 1997).

We have previously described the isolation of the RRM family protein, hermes, which is prominently expressed in the differentiating myocardium of the heart (Gerber *et al.*, 1999). Expression is also observed in the developing kidney and the ganglion layer of the retina. In each of these tissues, *hermes* expression is first detected at about the same time that markers of terminal differentiation are expressed (Gerber *et al.*, 1999). In this study, we describe experiments aimed at identifying the function of hermes during vertebrate development. First, we have utilized the *Xenopus* oocyte for experiments to determine subcellular localization of the hermes protein and to analyze protein–protein and protein–RNA interactions. Second, we demonstrate that temporal misexpression of *hermes* in the embryo completely eliminates myocardial differentiation and morphogenesis. Furthermore, misexpression in kidney primordia eliminates transcription of kidney markers. Although the mechanism remains unknown, our studies suggest that hermes regulates an aspect of mRNA metabolism necessary for cardiac and kidney differentiation.

MATERIALS AND METHODS

Oocyte Injections

Oocytes were manually defolliculated and then injected with 250 ng of *in vitro* transcribed mRNA. Capped mRNA was synthesized *in vitro* by using linearized hermes plasmid templates and the Message Machine *in vitro* transcription kit (Ambion). Oocytes were incubated at 18°C in OR2 (82.5 mM NaCl, 2.5 mM KCl, 1 mM $CaCl_2$, 1 mM $MgCl_2$, 1 mM Na_2HPO_4, 5 mM Hepes, pH 7.8) for 16–24 h then homogenized (25 μl/oocyte) in oocyte homogenization buffer (100 mM NaCl, 10 mM Tris–HCl, pH 7.6, 5 mM EDTA, 0.25% NP-40, 0.5 mM PMSF, and 1 mM DTT). Extracts were centrifuged for 4 min at 14,000*g* to remove yolk and pigment. For labeling of proteins, [^{35}S]methionine (NEN) was coinjected with the mRNA. For subcellular localization studies, the nucleus was manually removed and individually homogenized in 25 μl homogenization buffer.

Immunoprecipitation

Oocyte extracts equivalent to one-fifth of a single oocyte were incubated with 2 μl anti-HA polyclonal antibody (BAbCo) or 2 μl anti-myc 9E10 (Developmental Studies Hybridoma Bank, University of Iowa) and 40 μl protein-A agarose resin in 200 μl IP buffer (100 mM NaCl, 10 mM Tris–HCl, pH 7.5, 1 mM EDTA, 0.25% IGEPAL CA-630/NP-40), overnight at 4°C with gentle mixing. After precipitation, pellets were washed five times in ice-cold IP buffer. Pellets were then resuspended in SDS–PAGE loading buffer and fractionated on an SDS–PAGE gel containing 15% acrylamide.

Immunocytochemistry

Sections of MTHermes-injected oocytes were incubated in blocking buffer (1× PBS, 1% heat-treated lamb serum, 5% BSA) for 1 h at room temperature. The slides were incubated in a 1:200 dilution of anti-myc 9E10 monoclonal antibody (DSHB, University of Iowa) overnight at 4°C. Slides were washed three times in 1× PBS and then incubated for 2 h at room temperature, in the dark, in a 1:75 dilution of goat anti-mouse-FITC (Jackson Labs). Slides were again washed three times in 1× PBS and mounted in 100 nM Tris–HCl, pH 7.6, 80% glycerol, 1% *n*-propylgallate.

RNase protection

Total RNA was isolated from *Xenopus* embryos by homogenization in 4 M guanidinium thiocyanate, 25 mM sodium citrate, 0.5% sarkosyl, and 0.1 M β-mercaptoethanol, and the homogenate was phenol:chloroform extracted and then isopropanol precipitated. After resuspension in equal volumes of TE and 8 M LiCl, the RNA was recovered by centrifugation and then stored as an ethanol precipitate at −20°C. For RNase protection analysis, *hermes* transcripts were detected with a ^{32}P- labeled antisense probe consisting of sequences spanning nucleotides 459–773. Probe for XMax2 was prepared as described previously (Tonissen and Krieg, 1994).

Embryo Injections

Xenopus laevis embryos were generated by using standard techniques and staged according to Nieuwkoop and Faber (1994). Capped mRNAs were synthesized *in vitro* by using the Message Machine *in vitro* transcription kit (Ambion) and *Eco*RI-linearized pT7TS-hermes and *Not*I-linearized CS2+ vector (Turner and Weintraub, 1994) containing the green fluorescent protein (GFP)-coding region. Synthetic mRNAs encoding hermes and GFP were injected into one or both C1/C2 blastomeres to target the cardiac region, or into the C3 blastomere to target the pronephric region, of eight-cell embryos by using a Nanoject variable automatic injector (Drummond). In the standard protocol, 250 pg of hermes mRNA was injected with 250 pg of GFP mRNA as a lineage tracer in 4.6 nl of water. Injected embryos were cultured at 13°C in 4% Ficoll/0.4× MMR for 12 h and then in 0.2× MMR until stage 28, by which time heart differentiation has commenced.

Loss-of-function experiments were attempted by using antisense morpholino oligonucleotides (Gene Tools LLC). A combination of

two antisense oligonucleotides, AS1 (5′-CCGTGTCTGACTTGATGCCGCTCAT-3′) and AS2, (5′-GTACAAGCCAGACTCCTCGGTGGGC-3′) were used. These oligonucleotides are complementary to sequences overlapping the start site of translation and immediately upstream of the initiation ATG, respectively, and were designed to individually target both pseudoallelic copies of the *hermes* transcript. Each oligonucleotide was demonstrated to block translation of its respective target transcript when assayed in the reticulocyte lysate cell-free system. To target the heart region, a mixture of 8 ng of each morpholino oligonucleotide was injected into both C1/C2 blastomeres at the eight-cell stage by using the protocol described above. This represents a total of 32 ng of oligonucleotide per embryo. A control oligonucleotide RS1 (5′-TACTCGCCGTAGTTCAGTCTGTGCC-3′) representing the reverse of the first sequence above, and the standard control morpholino provided by Gene Tools were also injected at a final amount of 32 ng per embryo.

Poly(A)$^+$ Binding Assay

Oocyte extracts were prepared as described above, except that the homogenization buffer contained 8% glycerol, 50 mM NaCl, 2 mM $MgCl_2$, 5 mM BME, and 10 mM Tris–HCl, pH 7.6. After the initial centrifugation of the extracts, NaCl concentration was adjusted to 250 mM. The equivalent of 15 oocytes of extract was passed three times over a 0.3-ml (50 mg) oligo(dT) cellulose column (NE Biolabs) and then washed in five volumes of binding buffer (250 mM NaCl, 2 mM $MgCl_2$, 10 mM Tris–HCl, pH 7.6). Bound material was then eluted with 1.5 ml of 60% formamide. The eluate was precipitated with 3 volumes of ice-cold acetone and analyzed by SDS–PAGE.

Whole-Mount in Situ Hybridization

Digoxigenin-labeled RNA probes were prepared by using a MEGAscript kit (Ambion). Whole-mount *in situ* hybridization was carried out as previously described (Gerber *et al.*, 1999) and developed by using NBT-BCIP (Roche). Paraffin sections on embryos assayed by *in situ* hybridization were carried out by dehydrating the embryos in a graded ethanol series and washing twice for 20 min each in xylene and then three times in paraplast at 60°C for a total of 2 h. Embryos were then embedded in paraplast and sectioned at a thickness of 10 μm. Slides were dewaxed in xylene and viewed by DIC optics. When analyzing the phenotypes of injected embryos, statistical significance was determined by using the Student's *t* test with two-tailed, two sample unequal variance.

RESULTS

High Levels of hermes Transcript Are Present in the Xenopus Egg

Our original study used whole-mount *in situ* hybridization to determine the zygotic expression pattern of *hermes* (Gerber *et al.*, 1999). Using this protocol, *hermes* expression is first detected at stages 26–28, in the developing heart and kidney. However, when we further examined the *hermes* expression profile using RNase protection analysis, we found that *hermes* transcripts are also present at very high levels in the egg (Fig. 1). During cleavage and early development, this maternal stockpile of transcript declines significantly, but large amounts of maternal *hermes* RNA remain present through gastrulation (stage 10.5) and neurula stages (stage 16). By whole-mount *in situ* hybridization, tissue-specific expression of *hermes* becomes very clearly visible in the heart and kidney primordia between stages 26 and 28. In the RNase protection profile in Fig. 1, no significant increase in embryonic hermes transcript level is obvious at stage 26, but becomes evident by the tadpole stage (stage 36). Expression levels increase slightly throughout later development, consistent with the *in situ* hybridization results, but zygotic levels remain much lower than those observed in the egg. At present, it is not clear why the maternal *hermes* transcripts were not detected in our previous *in situ* hybridization studies, which showed a very clear, tissue-restricted expression pattern (Gerber *et al.*, 1999). It is possible, however, that broadly distributed *hermes* transcripts would be much less prominent than the same sequence expressed at high levels in a specific tissue.

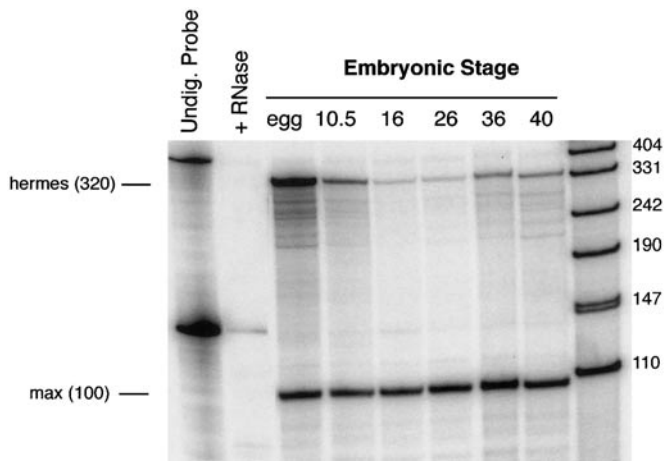

FIG. 1. Developmental expression of hermes. Total RNA was extracted from staged *X. laevis* embryos and analyzed by RNase protection. The equivalent of five embryos of total RNA was used for each sample. Embryonic stage is indicated at the top of the figure (Nieuwkoop and Faber, 1994). The position of the protected *hermes* and *Max* fragments, with the approximate nucleotide length in parentheses, is indicated on the left, and size markers are on the right. The *Max* sequence, which is expressed at constant levels throughout early development (Tonissen and Krieg, 1994), is used as a loading control.

Subcellular Localization in Oocytes

We have used two experimental methods to determine the subcellular localization of the hermes protein. Both experiments utilize the *Xenopus* oocyte, where the *hermes* transcript is normally expressed at high levels (Fig. 1). In the first approach, stage VI oocytes were coinjected with synthetic mRNA encoding wild-type hermes and with [^{35}S]methionine, to facilitate labeling of newly translated proteins.

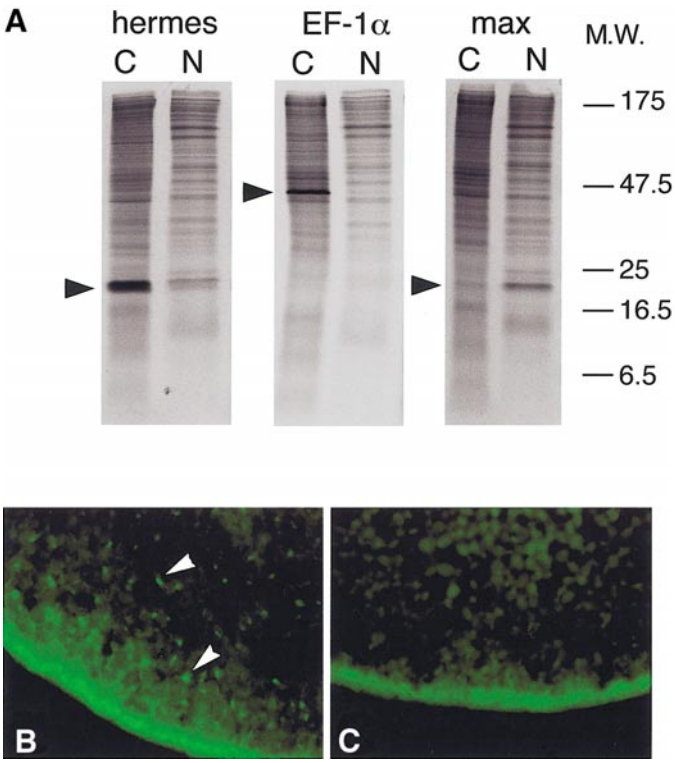

FIG. 2. Subcellular localization of hermes in the oocyte. (A) Hermes is present in both the nuclear and cytoplasmic compartments. Synthetic mRNAs encoding either hermes, the cytoplasmic protein EF-1α, or the nuclear protein Max were injected into the cytoplasm of *Xenopus* oocytes, together with [^{35}S]methionine. Oocytes were manually dissected into cytoplasmic (C) and nuclear (N) fractions. Protein extracts equivalent to one-fifth of each fraction from a single oocyte were resolved on SDS–PAGE and visualized by fluorography. Results indicate that the control proteins EF-1α and Max localize to the cytoplasmic and nuclear fractions, respectively. hermes is present primarily in the cytoplasm, but a small portion of hermes is found in the nuclear fraction. (B, C) Immunolocalization of epitope-tagged hermes protein in the oocyte. Synthetic mRNAs encoding myc-epitope-tagged proteins were injected into mature oocytes, and the resulting proteins were visualized by immunocytochemistry on sectioned oocytes. (B) View of the vegetal region of a MTHermes-injected oocyte. Staining appears as a punctate pattern. (C) View of the vegetal region of an oocyte expressing myc-epitope tag alone. Staining is diffuse and does not show the punctate pattern seen with MThermes.

After allowing radiolabeled protein to accumulate in the oocyte, the germinal vesicle (GV) was manually isolated and the cytoplasmic and GV fractions were analyzed by SDS–PAGE. As shown in Fig. 2A, hermes protein is present in both the nuclear and the cytoplasmic fractions. Quantitation of 10 individual oocytes shows that approximately 15% of hermes is present in the nucleus and 85% is cytoplasmic (SE ± 3%). In control experiments, the nuclear protein Max is 95% nuclear and 5% cytoplasmic, whereas the cytoplasmic protein EF-1α is 100% localized to the cytoplasm (Fig. 2A). The very clear partitioning observed for the EF-1α control indicates that the hermes protein detected in the nuclear fraction does not result from contamination of the GV sample with cytoplasmic material

In the second experiment, mature oocytes were injected with a synthetic mRNA encoding hermes protein carrying a myc-epitope tag or a control transcript encoding the myc-tag alone (see Fig. 3A). Subcellular localization of hermes protein was then visualized by immunofluorescence using an anti-myc antibody. The results of this assay also indicate that hermes protein is located in both the nucleus and the cytoplasm. In the nucleus and in the animal pole region, hermes protein appears to be evenly distributed, with no discernible localization to nuclear or cytoplasmic subregions (data not shown). However, in the vegetal region of the oocyte, the myc-tagged hermes protein appears to be associated with distinct granular structures (Fig. 2B). In contrast, oocytes injected with mRNA coding for the myc-epitope tag do not show granular staining in the vegetal cytoplasm (Fig. 2C). This punctate staining of Myc-tagged hermes protein in the vegetal region was observed in 11 of 14 oocytes examined, but was never observed in oocytes expressing the Myc-epitope tag alone (0 of 12 oocytes examined). We have also used immunofluorescence to examine localization of Myc-epitope-tagged hermes protein in the developing embryo until the tailbud stage. In these experiments, the majority of hermes protein was always observed in the cytoplasm, although a punctate pattern was not observed (data not shown). This suggests that no major change in the subcellular localization of hermes protein occurs during early embryogenesis.

Association of hermes Protein with Poly(A)$^+$ RNA in Vivo

In view of our results showing that hermes protein is localized predominantly to the cytoplasm (Fig. 2A), we wished to determine whether hermes could associate with poly(A)$^+$ RNA *in vivo*. To test this possibility, oocytes were injected with mRNA encoding different regions of the hermes protein, each carrying a myc-epitope tag (Fig. 3A). These constructions encode the full-length hermes protein, the RRM domain, or the C-terminal region. As a control, all oocytes were coinjected with mRNA encoding green fluorescent protein (GFP) which is not expected to exhibit any association with RNA within the cell. After allowing labeled hermes protein to accumulate, total oocyte extracts were prepared and then passed over an oligo(dT) cellulose column to determine whether hermes associates with poly(A)$^+$ RNA in the oocyte. The results of this experiment are presented in Figs. 3B and 3C. As shown in Fig. 3B, hermes is greatly enriched relative to the oocyte protein background and to the GFP control protein. Note that the labeled oocyte proteins in the oligo(dT)-bound fraction do not generally correspond to the labeled bands in the loaded material, suggesting that protein association with the column material is specific and not merely background bind-

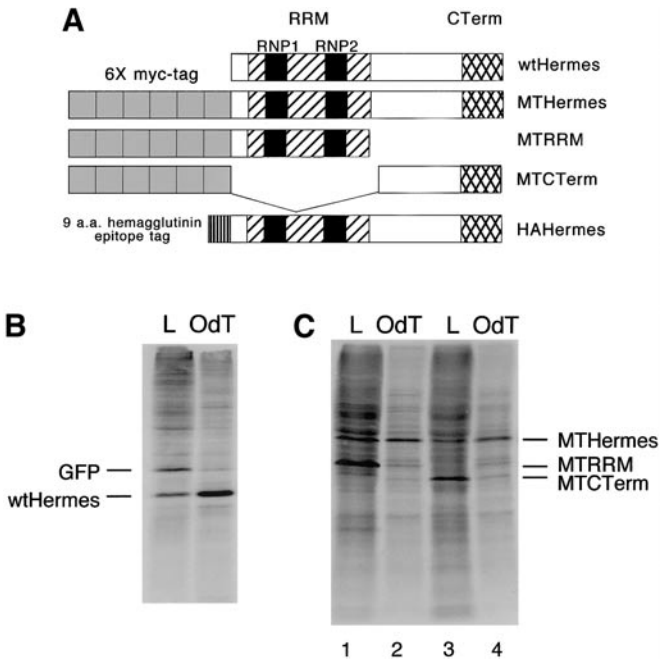

FIG. 3. Hermes associates with poly(A)$^+$ RNA *in vivo*. (A) Diagram depicting different hermes constructions used for protein and RNA interaction experiments. A 6xMyc epitope tag or a hemagglutinin (HA) tag was fused to the full-length hermes-coding region contained in T7TS. The myc epitope tag was also fused to subdomains of the hermes protein, containing either the first 100 amino acids (RRM), which includes the entire RNA-binding domain, or the last 97 amino acids (CTerm), which includes the highly conserved C-terminal end of the protein. (B, C) hermes associates preferentially with poly(A)$^+$ *in vivo*. (B) Extracts from oocytes injected with mRNA for GFP (a nonspecific control) and wtHermes and incubated with [^{35}S]methionine (L) were passaged over an oligo(dT) cellulose column. The bound fraction (OdT) is enriched for hermes protein relative to GFP, indicating an ability of hermes to associate with poly(A)$^+$ RNA. (C) Repeat of the experiment in (B), except oocytes were injected with combinations of mRNA for MThermes (as a positive control) and mRNA for MTRRM (lanes 1 and 2) or MTCTerm (lanes 3 and 4) in order to determine which domains of the protein are necessary for the poly(A)$^+$ interaction. Only the MTHermes is enriched in the bound fraction, indicating that both the RRM and CTerm are necessary for association with poly(A)$^+$ RNA.

ing. Quantitation of three different experiments shows that hermes is approximately 10-fold enriched in the poly(A)$^+$ fraction relative to GFP. When deletion constructions of hermes are tested, only the full-length hermes protein associates with poly(A)$^+$ RNA (Fig. 3C). Neither the RRM domain (MTRRM) or the C-terminal portion (MTCTerm) of the hermes protein associates significantly, suggesting that both domains are necessary for interaction with mature mRNA. In separate experiments, we have attempted to determine whether hermes protein translated in a reticulocyte lysate can associate with RNA. Numerous experiments using different target RNA populations and different binding conditions failed to show any association of hermes protein with RNA *in vitro*. Possible explanations for this observation will be discussed later.

Protein–Protein Interactions

Many RNA-binding proteins, particularly those containing a single RNA-binding motif, function as homodimers or homo-oligomers (Zorn and Krieg, 1997; Wang *et al.*, 1999; reviewed in Siomi and Dreyfuss, 1997). In order to determine whether hermes is capable of homodimerization *in vivo*, we carried out coimmunoprecipitation experiments using *Xenopus* oocyte extracts. Mature oocytes were injected with synthetic mRNAs encoding HA-epitope tagged and untagged versions of hermes (Fig. 3A) together with [^{35}S]methionine. Oocyte extracts were prepared and immunoprecipitation was carried out by using anti-HA antibody. These experiments show that wild-type hermes protein coprecipitates with HA-tagged hermes (Fig. 4A), suggesting that hermes forms dimers or multimers in the oocyte. However, since hermes is an RNA-binding protein, this coimmunoprecipitation result is not necessarily straightforward to interpret. Indeed, the observed coimmunoprecipitation of hermes proteins is consistent, both with direct protein–protein interactions, and also with a situation where hermes protein is binding in multiple monomeric units along a single RNA molecule. To test this latter possibility, oocyte extracts were treated with RNase prior to immunoprecipitation. As shown in Fig. 4A, RNase treatment reduces but does not completely eliminate coprecipitation. Quantitation of this effect over five different experiments shows that immunoprecipitation of untagged hermes is reduced to approximately one-quarter of normal levels by RNase treatment (27%, SE ± 4%). The hermes protein association remaining after RNase treatment may be because a small proportion of the hermes protein is involved in direct protein/protein interactions, or because other bound proteins protect the RNA molecule from further RNase degradation. Nevertheless, we conclude from these experiments that the interaction of hermes proteins seen in immunoprecipitation experiments is at least partly dependent on RNA. In order to determine which portions of the hermes protein participate in this interaction, we injected oocytes with mRNA encoding either the RRM (MTRRM) or the C-terminal (MTCTerm) portions of hermes together with untagged wild-type hermes. The results of the immunoprecipitation experiments show that neither of these subdomains is sufficient for stable interactions with untagged hermes, either directly or through indirect associations with RNA (Fig. 4B). This result is consistent with the oligo(dT)-binding experiments, which showed that full-length hermes protein is required for association with poly(A)$^+$ RNA (Fig. 3B).

Misexpression of hermes in the Embryo Compromises Heart Differentiation

During *Xenopus* development, one of the earliest regions showing tissue-restricted expression of *hermes* is the em-

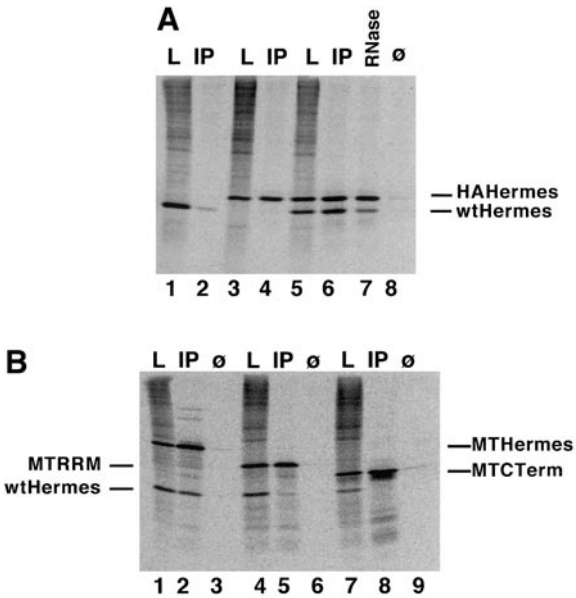

FIG. 4. Hermes protein–protein interactions. (A) Immunoprecipitation experiment showing that the ability of hermes proteins to complex *in vivo* is RNase-sensitive. Lanes 1 and 2, extracts from oocytes injected with mRNA for untagged, wild-type hermes. Lanes 3 and 4, extracts from oocytes injected with mRNA for only HA-tagged hermes. Lanes 5–8, extracts from oocytes injected with mRNA for both HA-tagged and untagged, wild-type hermes. Lanes 5–8 show that coimmunoprecipitation of hermes proteins is sensitive to RNase. (B) Immunoprecipitation experiments showing that both the RRM and C-terminal region are required for the coimmunoprecipitation of hermes. Lanes 1–3, extracts from oocytes injected with mRNA for MTHermes and wtHermes. Lanes 5 and 6, extracts from oocytes injected with mRNA for MTRRM and wtHermes. Lanes 7–9, extracts from oocytes injected with mRNA for MTCTerm and wtHermes. Lane marked "L" contains 20% of total material used in the immunoprecipitation reaction. IP, immunoprecipitation with anti-HA or anti-myc antibody. RNase, treatment of extracts with RNase prior to immunoprecipitation. Lane marked "ø" is immunoprecipitation without antibody.

bryonic heart. Heart expression of *hermes* is first detected between stages 26 and 28, which corresponds to the time of heart differentiation, as assayed by expression of cardiac muscle markers such as *cardiac α-actin* and *cardiac troponin I* (Hemmati-Brivanlou *et al.,* 1990; Drysdale *et al.,* 1994). This correlation suggests that hermes may play a role in regulation of transcripts involved in cardiac differentiation. To investigate a possible function for hermes during heart development, we have used microinjection to temporally misexpress hermes in the *Xenopus* embryo. We have principally focused on development of the heart, rather than other tissues, due to the availability of a number of well-characterized pre- and postdifferentiation cardiac markers. In initial experiments, 250 pg of *hermes* mRNA, together with mRNA encoding GFP lineage tracer was injected into a C1/C2 blastomere, in order to concentrate hermes expression in the future heart-forming region (Dale and Slack, 1987; Moody, 1987). Embryos injected with 250 pg of *hermes* mRNA appeared generally normal through all stages of early development, indicating that the presence of excess hermes protein does not cause nonspecific toxic effects on embryogenesis. At stage 28/29, embryos showing the presence of GFP lineage tracer in the heart were analyzed for expression of myocardial markers by whole-mount *in situ* hybridization. Initial analyses were carried out by using the heart differentiation marker, *cardiac troponin I* (*TnIc*), which is specifically expressed in cardiac muscle (Drysdale *et al.,* 1994). As summarized in Table 1, expression of *TnIc* was greatly reduced or absent on the injected side of 46% of all embryos analyzed ($P < 0.005$). As a control, we injected mRNA encoding ΔRNP1, a mutated form of hermes that lacks seven amino acids from the highly conserved RNP1 of the RRM. Previous studies indicate that mutations of the RNP1 region effectively eliminate sequence-specific RNA binding (Heinrichs and Baker, 1997). Our results indicate that expression of ΔRNP1 in the heart region of the embryo has no statistically significant effect on *TnIc* expression (Table 1). This observation implies that sequence-specific binding is essential for the hermes overexpression phenotype.

In order to obtain additional information on the specificity of the hermes misexpression phenotype, a more extensive series of assays were carried out by using probe for *cardiac α-actin*, which is expressed in both cardiac and somitic muscle (Mohun *et al.,* 1988). When the C1/C2 blastomeres are injected, embryos with lineage tracer in the heart region always contain tracer in the anterior somites on the injected side, because these blastomeres contribute to both lineages (Dale and Slack, 1987; Moody, 1987). Use of *cardiac α-actin* probe, therefore, permits analysis of the effects of hermes overexpression on both heart and somite muscle development. Results of these experiments are presented in Fig. 5. As expected, embryos injected with GFP alone show normal morphology and bilaterally symmetrical expression of *cardiac α-actin* in the developing heart

TABLE 1

Asymmetry of Expression of *cardiac troponin I* in *hermes* Injected Embryos

Injected construct	Total (n)	% Asymmetry
Hermes + GFP	216	46%
GFP	147	5%
MTΔRNP1 + GFP	33	3%

Note. 250 pg of *hermes* mRNA construct, together with 250 pg of mRNA encoding GFP lineage tracer was injected into the future heart-forming region of the embryo at the 4–8-cell stage and assayed at stage 28/29. Only embryos expressing GFP tracer in the heart region were included in this assay. Embryos were scored positive for asymmetry if cardiac troponin expression was absent or nearly absent on the injected side of the embryo. 250 pg of *MTΔRNP1,* injected as a control, represents a mutated form of *hermes* that eliminates RNA sequence specific binding.

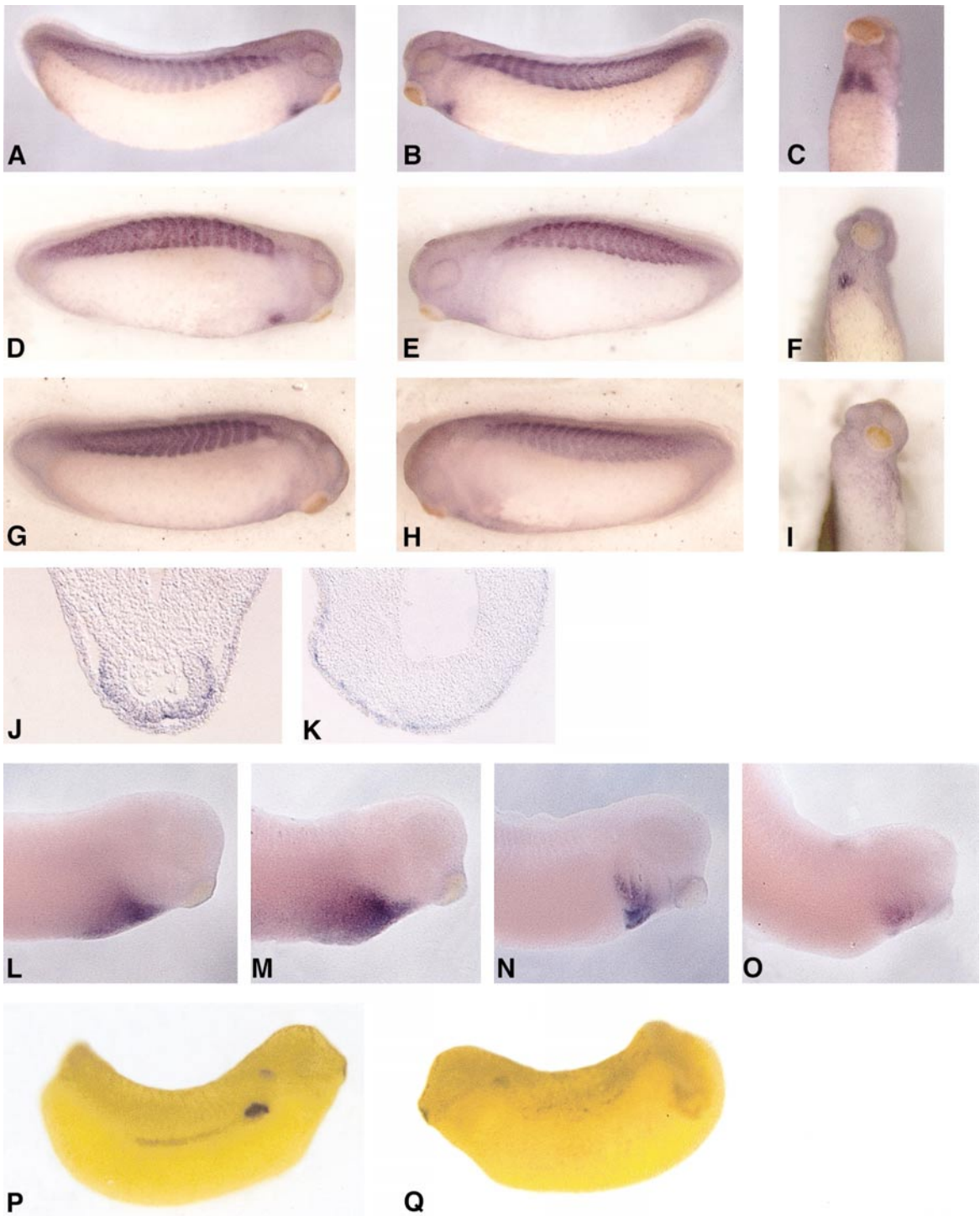

FIG. 5. Overexpression of hermes inhibits heart and kidney development. Embryos injected with mRNA encoding hermes and lineage tracer GFP, or GFP alone. All embryos are at stage 28/29, unless otherwise specified. Whole-mount *in situ* hybridizations are photographed as lateral views except for (C), (F), and (I), which are ventral views of the same embryos pictured laterally. (A–C) GFP-injected control embryos showing normal expression of *cardiac α-actin* in the somites (A, B) and paired heart primordia (C). (D–F) Single-sided injections cause the ablation of the heart-forming region on the injected side (arrow) as assayed by *cardiac α-actin*. (G–I) Double-sided injections showing complete ablation of both heart primordia, while somite morphology (G, H) is unperturbed as assayed by *cardiac α-actin*. (J, K) Transverse sections through stage 32 embryos (linear heart tube stage) injected with GFP mRNA only (J) or bilaterally injected with *hermes* mRNA (K) and assayed by *cardiac α-actin*. Note the absence of any *cardiac α-actin* staining as well as the absence of a morphologically detectable heart tube in (K), although the heart tube is easily detectable in (J). (L, M) *GATA-4* expression in control embryos (L) is indistinguishable from *hermes*-injected embryos (M). (N, O) By contrast, a *hermes*-injected embryo (O) has reduced *Nkx2–5* expression compared with a control GFP-injected embryo (N). (P, Q) A stage 25 *hermes*-injected embryo assayed with the kidney marker *X-pax2*. The uninjected side (P) shows normal kidney expression, while the injected side (Q) shows the absence of all kidney expression.

region (Figs. 5A–5C). Embryos overexpressing hermes show generally normal overall morphology, except for a slightly bulbous appearance. *In situ* analysis reveals that embryos overexpressing hermes show a dramatic reduction in *cardiac α-actin* expression in the developing heart region (Figs. 5D–5F). Importantly, *cardiac α-actin* expression in the somites is normal on both the injected and the uninjected sides of the embryo, indicating that the presence of hermes is not influencing development of somitic muscle markers. As shown in Figs. 5G–5I, bilateral injection of 250 pg of *hermes* mRNA into both the C1 and C2 blastomeres completely eliminated cardiac α-actin expression in both heart patches. Total absence of marker expression was observed in 30% of injected embryos (9/30), and marked reduction in one of the heart patches was observed in an additional 53% of the embryos (16/30). When compared with controls, these differences are highly statistically significant ($P < 0.005$). In order to examine the effects of hermes misexpression on heart morphology, bilaterally injected embryos were allowed to develop until stage 32, when the heart normally forms a simple linear tube (Mohun *et al.*, 2000; Kolker *et al.*, 2000). Histological sections show that embryos lacking expression of cardiac α-actin in the precardiac region also fail to form a morphologically distinguishable heart tube (see Figs. 5J and 5K).

The experiments so far have focused on heart muscle differentiation markers, but it is possible that hermes misexpression interferes with the normal expression of regulatory molecules expressed prior to cardiac differentiation. To test this possibility, hermes-overexpressing embryos were assayed with probes for the cardiac regulatory genes *Nkx2–5* and *GATA-4*. Analysis of these embryos showed that *GATA-4* expression was largely unaltered in tailbud stage embryos expressing hermes mRNA. Only 15% (7/45) of double side-injected embryos showed a detectable reduction in *GATA-4* expression in the precardiac region, which is not significantly different when compared to controls. This is much less than the 83% reduction or elimination observed when the same batch of embryos was assayed for cardiac α-actin expression. In contrast, however, analysis of tailbud embryos from the same batch shows that *Nkx2–5* expression is strongly reduced in 53% (26/57) of *hermes*-overexpressing embryos (compare Fig. 5N with 5O), which is significantly different than control embryos ($P < 0.005$). Overall, these experiments suggest that misexpression of hermes may be blocking expression of cardiac differentiation markers by interfering with an upstream regulator of cardiac development, possibly Nkx2–5.

In addition to expression in developing heart tissue, *hermes* is also strongly expressed in the developing kidney. We have carried out a preliminary series of experiments to determine whether misexpression of hermes might also interfere with kidney development. In these experiments, 250 pg of *hermes* was injected into a C3 blastomere that is fated to contribute to pronephros and somite (Dale and Slack, 1987). Since there are few established markers for kidney differentiation, our assays were carried out by using the predifferentiation marker *Xpax-2*, which is expressed at high levels throughout developing kidney tissues (Heller and Brändli, 1997; Carroll *et al.*, 1999). As shown in Figs. 5P and 5Q, misexpression of *hermes* causes a severe reduction or ablation of *Xpax-2* expression. This was observed in 36% of injected embryos (9/26), which is statistically different from the 5% of GFP control injected embryos (1/19) ($P = 0.01$). To confirm that hermes expression is not producing nonspecific toxic effects, a proportion of the same batch of embryos was assayed with *cardiac α-actin* probe to examine somite development. In all cases, somite appearance on the injected side of the embryo was indistinguishable from that on the uninjected side (data not shown). This result is particularly relevant because the developing kidney and the somites are in immediate proximity to each other. We conclude from these preliminary studies that misexpression of *hermes* interferes with kidney development while leaving muscle gene expression in the somites, and overall somite morphology, unaffected.

Morpholino Oligonucleotide Experiments

In addition to assaying for the effects of overexpression of hermes, we attempted loss/reduction-of-function studies using morpholino antisense oligonucleotides directed against the hermes transcripts. A total of 32 ng of oligonucleotide was targeted to the heart-forming region of the embryo, and assays for heart gene expression and overall heart morphology were carried out at stage 35, using *in situ* hybridization with cardiac probes followed by histological sectioning. The overall appearance of the oligonucleotide-injected embryos was indistinguishable from uninjected controls, suggesting that the presence of morpholino oligonucleotides was not producing general toxic effects. Prior to fixation for *in situ* hybridization, however, we noted that a proportion of the hearts in antisense morpholino-injected embryos were not beating or were beating slowly. Moreover, *in situ* hybridization analysis with the general muscle marker, *tropomyosin*, revealed morphological defects, including failure of the heart tube to loop correctly and disruption of the myocardial tissue layer (data not shown). Unexpected results, however, were obtained from embryos injected with control morpholino oligonucleotides. Although the control sequence provided by Gene Tools produced no detectable phenotype, the reverse sequence control, RS1, generated heart phenotypes indistinguishable from those produced with the antisense hermes morpholino oligonucleotides, namely absence of heartbeat and morphological defects in the heart tube. We conclude, therefore, that the phenotype produced by the hermes antisense oligonucleotides is artifactual. These results serve as a warning that morpholino oligonucleotides may disrupt heart formation, even when the overall development of the embryo appears normal. The mechanism responsible for these defects is currently unknown.

DISCUSSION

Hermes Is Present in Both the Cytoplasm and the Nucleus

To learn more about the possible function of hermes, we have determined the subcellular localization of the hermes protein. Using the oocyte as a model system, we have shown that hermes is primarily cytoplasmic, although a small proportion of the total protein (approximately 15%) is routinely detected in the nucleus. While the proportion of the total hermes protein in the nucleus is small, it is significantly greater than would be expected if hermes protein was freely diffusible, since the volume of the oocyte nucleus only represents about 3% of the volume of the entire cell. In addition, immunofluorescence studies show that cytoplasmic hermes is concentrated in granular structures, which are especially conspicuous near the vegetal cortex (Fig. 2B). These punctate structures are never observed in control oocytes. The appearance of these structures in the oocyte is similar to that previously reported for Vera, a protein associated with Vg1 mRNA (Deshler *et al.*, 1997), or for the cortical localized rough endoplasmic reticulum (RER), as revealed by an antibody directed against TRAPα (Hartmann *et al.*, 1993). These observations are consistent with a role for hermes in translational regulation of cortically localized messages in the oocyte.

Previous studies have shown that other RNA-binding proteins are also present in both the nucleus and cytoplasm. These include elav, an RRM-family protein required for neuronal differentiation (Perron *et al.*, 1997, 1999), boule, a *Drosophila* DAZL-related protein (Cheng *et al.*, 1998), the human poly(A)-binding protein 1 (Afonina *et al.*, 1998), FMR1, the protein involved in human fragile-X syndrome (Tamanini *et al.*, 1999), and SEB-4, an RRM-family protein expressed in *Xenopus* muscle tissue (Fetka *et al.*, 2000). Furthermore, it has been demonstrated that RNA-binding proteins can exhibit different functions in different cellular compartments. One prominent example is sex lethal, which regulates splicing in the nucleus, but is involved in translational repression in the cytoplasm (Bell *et al.*, 1988; Bashaw and Baker, 1997; Kelley *et al.*, 1997). Although we cannot rule out a role for hermes in the nucleus (e.g., splicing regulation), the fact that most hermes protein is located in the cytoplasm suggests a role in regulating mature mRNA, perhaps by regulating translation or message stability. This possibility is further supported by the observation that hermes protein is preferentially associated with poly(A)$^+$ RNA *in vivo* (Fig. 3B). The discovery that hermes is expressed at high levels in the oocyte (Fig. 1) is certainly consistent with hermes playing a role in regulation of transcript stability, since the oocyte contains a very large number of stored, stable mRNAs (Stebbins-Boaz and Richter, 1997; Mowry and Cote, 1999)

Homodimerization of hermes Is RNA-Dependent

Previous studies have shown that RNA-binding proteins often need to assemble into multiprotein complexes in order to bind RNA efficiently (Nelson and Green, 1989; Ruskin *et al.*, 1988; Siomi and Dreyfuss, 1997). These associations can be homodimers, heterodimers, or multimeric complexes. Our immunoprecipitation experiments indicate that multiple copies of the hermes protein are associated with each other within the cell (Fig. 4). The fact that the association of hermes proteins is sensitive to RNase suggests that it is not a simple protein/protein interaction. One possible explanation is that multiple copies of hermes protein may be binding to a single RNA molecule. In this case, there need be no physical interaction between individual hermes proteins. The second possibility is that RNA association is required for a conformational change in the hermes protein. This conformational change may allow association of hermes with other proteins (homo-oligomerization or hetero-oligomerization). Many RNA-binding proteins contain multiple RNA-binding modules (sometimes of different classes), and these multiple domains are important for efficient interaction with the target RNA (Burd and Dreyfuss, 1994). Since hermes contains only a single RNA-binding domain, it is plausible that hermes, like some other RNA-binding proteins, requires a cofactor in order to bind RNA efficiently. For example, U2 snRNP cannot bind to its target RNA unless the necessary cofactor, U2AF, is present (Nelson and Green, 1989; Ruskin *et al.*, 1988). The possibility that a protein cofactor is required for hermes to bind RNA efficiently may explain why neither protein–protein interactions nor protein–RNA interactions are observed by using hermes protein that has been translated *in vitro*. On the other hand, the necessary cofactor proteins are quite likely to be present in the oocyte, where hermes is normally expressed.

Misexpression of hermes Reveals a Role in Cardiac Differentiation

To determine a possible role for hermes during cardiac development, we have carried out experiments in which hermes is expressed at both an earlier time and higher levels than in normal development. These experiments demonstrate that embryos overexpressing hermes show greatly reduced expression of myocardial differentiation markers, including *TnIc* and *cardiac* α*-actin* (Fig. 5). Parallel experiments also showed a strong downregulation of the kidney predifferentiation marker, *Xpax-2*. The fact that somite development is normal in these embryos shows that hermes overexpression is interfering with development of specific tissues rather than causing general toxic effects. An important clue to the possible role of hermes during cardiac development comes from examination of expression of precardiac markers, such as *Nkx2–5* and *GATA-4*. These experiments indicate that expression of the early cardiogenic marker, *Nkx2–5*, is significantly reduced in response to hermes overexpression, whereas the levels of transcript-

encoding *GATA-4* are unaffected (Fig. 5; and Table 1). This result is important because it shows that hermes overexpression is not inhibiting cardiac development nonspecifically, but is reducing the expression of a subset of genes required for normal cardiogenesis. Since Nkx2–5 is an important regulator of numerous cardiac regulatory factors and differentiation (Lyons *et al.*, 1995; Tanaka *et al.*, 1999), it is plausible that the absence of cardiac marker expression in hermes-overexpressing embryos is caused by the downregulation of Nkx2–5 expression. It is important to note, however, that the reduction in Nkx2–5 transcript levels could be achieved by many different mechanisms, and we have no evidence suggesting that Nkx2–5 transcripts are a direct target of hermes binding.

In the *Xenopus* embryo, cardiac expression of *hermes* is first detected at the same time that heart differentiation markers are initially expressed (Gerber *et al.*, 1999). It is possible that the normal function of hermes is to modulate the transition from the precardiac to the cardiac differentiated state, perhaps by altering the expression of other regulatory molecules. This is consistent with our observation that hermes expression downregulated *Nkx2–5* in the tailbud embryo. The observation that hermes misexpression alters heart and kidney development while leaving somitic muscle development unchanged might be explained, either by the presence of specific accessory proteins in the cardiac and kidney tissue, or perhaps by sequence-specific binding. In the latter case, specific RNA targets of hermes binding may not be present in somitic tissue. Answers to these questions will probably depend on identification of the specific transcripts that are bound and regulated by the hermes protein. In summary, although the targets of hermes regulation are currently unknown, the observation that hermes overexpression leads to loss of expression of heart markers suggests that hermes functions in an essential pathway during cardiac development.

ACKNOWLEDGMENTS

We thank Larry Etkin for generously providing morpholino antisense oligonucleotides, Tom Carroll for providing the *Xpax-2* construct, and Todd Evans for the *GATA-4* construct. We also thank Parker Antin and Eric Small for comments on the manuscript and Larry Etkin for making information available prior to publication. P.A.K. is the Allan C. Hudson and Helen Lovaas Endowed Professor of the Sarver Heart Center at the University of Arizona College of Medicine. This research was supported by NHLBI, NIH Grant #HL63926 (to P.A.K.).

REFERENCES

Afonina, E., Stauber, R., and Pavlakis, G. N. (1998). The human poly(A)-binding protein shuttles between the nucleus and the cytoplasm. *J. Biol. Chem.* **273,** 13015–13021.

Antic, D., and Keene, J. D. (1997). Embryonic lethal abnormal visual RNA-binding proteins involved in growth, differentiation and posttranscriptional gene expression. *Am. J. Hum. Genet.* **61,** 273–278.

Antic, D., Lu, N., and Keene, J. D. (1999). Elav tumor antigen, Hel-N1, increases translation of neurofilament M mRNA and induces formation of neurites in human tetracarcinoma cells. *Genes Dev.* **13,** 449–461.

Bashaw, G. J., and Baker, B. S. (1997). The regulation of the *Drosophila msl-2* gene reveals a function for Sex-lethal in translational control. *Cell* **89,** 789–798.

Bell, L. R., Maine, E. M., Schedl, P., and Cline, T. W. (1988). *Sex-lethal*, a *Drosophila* sex determination switch gene, exhibits sex-specific RNA splicing and sequence similarity to RNA binding proteins. *Cell* **55,** 1037–1046.

Bodmer, R., and Venkatesh, T. V. (1998). Heart development in *Drosophila* and vertebrates: Conservation of molecular mechanisms. *Dev. Genet.* **22,** 181–186.

Burd, C. G., and Dreyfuss, G. (1994). Conserved structures and diversity of functions of RNA-binding proteins. *Science* **265,** 615–621.

Carroll, T. J., Wallingford, J. B., and Vize, P. D. (1999). Dynamic patterns of gene expression in the developing pronephros of *Xenopus laevis*. *Dev. Genet.* **24,** 199–207.

Cheng, M. H., Maines, J. Z., and Wasserman, S. A. (1998). Biphasic subcellular localization of the DAZL-related protein boule in *Drosophila* spermatogenesis. *Dev. Biol.* **204,** 567–576.

Curtis, D. (1994). Translational repression as a conserved mechanism for the regulation of embryonic polarity. *BioEssays* **16,** 709–711.

Dale, L., and Slack, J. M. W. (1987). Fate map for the 32 cell stage of *Xenopus laevis*. *Development* **99,** 527–551.

Deshler, J. O., Highett, M. I., and Schnapp, B. J. (1997). Localization of *Xenopus* Vg1 mRNA by Vera protein and the endoplasmic reticulum. *Science* **276,** 1128–1131.

Drysdale, T. A., Tonissen, K. F., Patterson, K. D., Crawford, M. J., and Krieg, P. A. (1994). Cardiac Troponin I is a heart specific marker in the *Xenopus* embryo: Expression during abnormal heart development. *Dev. Biol.* **165,** 432–441.

Ebersole, T. A., Chen, Q., Justice, M. J., and Artzt, K. (1996). The quaking gene product necessary in embryogenesis and myelination combines features of RNA binding and signal transduction proteins. *Nat. Genet.* **12,** 260–265.

Evans, S. M. (1999). Vertebrate tinman homologues and cardiac differentiation. *Semin. Cell Dev. Biol.* **10,** 73–83.

Fetka, I., Radeghieri, A., and Bouwmeester, T. (2000). Expression of the RNA recognition motif-containing protein SEB-4 during Xenopus embryonic development. *Mech. Dev.* **94,** 283–286.

Gerber, W., Yatskievych, T., Antin, P., Correia, K., Conlon, R., and Krieg, P. (1999). The RNA-binding protein gene, *hermes*, is expressed at high levels in the developing heart. *Mech. Dev.* **80,** 77–86.

Grunert, S., and St. Johnson, D. (1996). RNA localization and the development of asymmetry during Drosophila oogenesis. *Curr. Opin. Genet. Dev.* **6,** 395–402.

Hardy, S., Fiszman, M. Y., Osborne, H. B., and Thiebaud, P. (1991). Characterization of muscle and non muscle *Xenopus laevis* tropomyosin mRNAs transcribed from the same gene. Developmental and tissue-specific expression. *Eur. J. Biochem.* **202,** 431–440.

Hartmann, E., Gorlich, D., Kostka, S., Otto, A., Kraft, R., Knespel, S., Burger, E., Rapoport, T. A., and Prehn, S. (1993). A tetrameric complex of membrane proteins in the endoplasmic reticulum. *Eur. J. Biochem.* **214,** 375–381.

Harvey, R. P., Biben, C., and Elliott, D. A. (1999). Transcriptional control and pattern formation in the developing vertebrate heart: Studies on NK-2 class homeodomain factors. In "Heart Development" (R. P. Harvey and N. Rosenthal, Eds.), pp. 111–129. Academic Press, San Diego.

Hauberman, B., Mi, H. F., Edelmann, A., Bohring, C., Backert, I. T., Kiesewetter, F., Aumuller, G., and Vogt, P. H. (1998). DAZ (Deleted in AZoospermia) genes encode proteins located in human late spermatids and in sperm tails. *Hum. Reprod.* **13,** 363–369.

Heasman, J., Kofron, M., and Wylie, C. (2000). β-Catenin signaling activity dissected in the early *Xenopus* embryo: A novel antisense approach. *Dev. Biol.* **222,** 124–134.

Heinrichs, V., and Baker, B. S. (1997). In vivo analysis of the functional domains of the Drosophila splicing regulator RBP1. *Proc. Natl. Acad. Sci. USA* **94,** 115–120.

Heller, N., and Brändli, A. (1997). *Xenopus* Pax-2 displays multiple splice forms during embryogenesis and pronephric kidney development. *Mech. Dev.* **69,** 83–104.

Hemmati-Brivanlou, A. Frank, D., Bolce, M. E., Brown, B. D., Sive, H. L., and Harland, R. M. (1990). Localization of specific mRNAs in *Xenopus* embryos by whole-mount in situ hybridization. *Development* **110,**325–330.

Hoffman, D. W., Query, C. C., Golden, B. L., White, S. W., and Keene, J. D. (1991). RNA-binding protein domain of the A protein component of the U1 small nuclear ribonucleoprotein analyzed by NMR spectroscopy is structurally similar to ribosomal proteins. *Proc. Natl. Acad. Sci. USA* **88,** 2495–2499.

Kaufmann, W. E., and Reiss, A. L. (1999). Molecular and cellular genetics of fragile-X syndrome. *Am J. Med. Genet.* **88,** 11–24.

Kelley, R. L., Wang, J., Bell, L., and Kuroda, M. I. (1997). Sex lethal controls dosage compensation in *Drosophila* by a non-splicing mechanism. *Nature* **387,** 195–199.

Kolker, S. J., Tajchman, U., and Weeks, D. L. (2000). Confocal imaging of early heart development in *Xenopus laevis*. *Dev. Biol.* **218,** 64–73.

Koushika, S. P., Lisbin, M. J., and White, K. (1996). ELAV, a *Drosophila* neuron-specific protein, mediates the generation of an alternatively spliced neural protein isoform. *Curr. Biol.* **6,** 1634–1641.

Liu, J., Beqaj, S., Yang, Y, Honore, B., and Schuger, L. (2001). Heterogeneous nuclear ribonucleoprotein-H plays a suppressive role in visceral myogenesis. *Mech. Dev.* **104,** 79–87.

Logan, M., and Mohun, T. (1993). Induction of cardiac muscle differentiation in isolated animal pole explants of *Xenopus laevis* embryos. *Dev. Biol.* **118,** 865–875.

Lyons, I., Parson, L. M., Hartley, L., Li, R., Andrews, J. E., Robb, L., and Harvey, R. P. (1995). Myogenic and morphogenetic defects in the heart tubes of murine embryos lacking the homeo box gene Nkx2–5. *Genes Dev.* **9,** 1654–1666.

Mohun, T. J., Garrett, N., Stutz, F., and Spohr, G. (1988). A third striated muscle actin gene is expressed during early development in the amphibian *Xenopus laevis*. *J. Mol. Biol.* **202,** 67–76.

Mohun, T. J., Leong, L. M., Weninger, W. J., and Sparrow, D. B. (2000). The morphology of heart development in *Xenopus laevis*. *Dev. Biol.* **218,** 74–88.

Moody, S. A. (1987). Fates of the blastomeres of the 32-cell-stage *Xenopus* embryo. *Dev. Biol.* **122,** 300–319.

Mowry, K. L., and Cote, C. A. (1999). RNA sorting in *Xenopus* oocytes and embryos. *FASEB J.* **13,** 435–445.

Nagai, K., Oubridge, C., Jessen, T. H., Li. J., and Evans, P. R. (1990). Crystal structure of the RNA-binding domain of the U1 small nuclear ribonucleoprotein A. *Nature* **348,** 515–520.

Nelson, K. K., and Green, M. R. (1989). Mammalian U2 snRNP has a sequence-specific RNA-binding activity. *Genes Dev.* **3,** 1562–1571.

Nieuwkoop, P. D., and Faber, J. (1994). "Normal Table of *Xenopus laevis* (Daudin): A Systematical and Chronological Survey of the Development from the Fertilized Egg till the End of Metamorphosis." Garland Publishing, Inc., New York.

Olson, E. N. (2001). The path to the heart and the road not taken. *Science* **291,** 2327–2328.

Perron, M., Bourlitio, P., Wegnez, M., and Theodore, L. (1997). Subcellular distribution of *Xenopus* XEL-1 protein, a member of the neuron-specific ELAV/Hu family, revealed by epitope-tagging. *DNA Cell Biol.* **16,** 579–587.

Perron, M., Furrer, M-P., Wegnez, M., and Theodore, L. (1999). Xenopus elav-like genes are differentially expressed during neurogenesis. *Mech. Dev.* **84,** 139–142.

Robinow, S., Campos, A. R., Yao, K. M., and White K. (1988). The elav gene product of *Drosophila*, required in neurons, has three RNP consensus motifs. *Science* **242,** 1570–1572.

Ruskin, B., Zamore, P. D., and Green, M. R. (1988). A factor, U2AF, is required for U2 snRNP binding and splicing complex assembly. *Cell* **29,** 207–219.

Schumacher, J. M., Artzt, K., and Braun, R. E. (1998). Spermatid perinuclear ribonucleic acid-binding protein binds microtubules in vitro and associates with abnormal manchettes in vivo in mice. *Biol. Reprod.* **1,** 69–76.

Siomi, H., and Dreyfuss, G. (1997). RNA-binding proteins as regulators of gene expression. *Curr. Opin. Genet. Dev.* **7,** 345–353.

Stebbins-Boaz, B., and Richter, J. D. (1997). Translational control during early development. *Crit. Rev. Eukaryot. Gene Expr.* **7,** 73–94.

Tamanini, F., Bontekoe, C., Bakker, C. E., van Unen, L., Anar, B., Willemsen, R., Yoshida, M., Galjaard, H., Oostra, B. A., and Hoogeveen, A. T. (1999). Different targets for the fragile X-related proteins revealed by their distinct nuclear localizations. *Hum. Mol. Genet.* **8,** 863–869.

Tanaka, M., Chen, Z., Bartunkova, S., Yamasaki, N., and Izumo, S. (1999). The cardiac homeobox gene Csx/Nkx2–5 lies genetically upstream of multiple genes essential for heart development. *Development* **126,** 1269–1280.

Tonissen, K. D., and Krieg, P. A. (1994). Analysis of a variant Max sequence expressed in *Xenopus laevis*. *Oncogene* **9,** 33–38.

Turner, D. L., and Weintraub, H. (1994). Expression of achaete-scute homolog 3 in *Xenopus* embryos converts ectodermal cells to a neural fate. *Genes Dev.* **8,** 1311–1323.

Wang, W., Riedel, K., Lynch, P., Chien, C. Y., Montelione, G. T., and Krug, R. M. (1999). RNA binding by the novel helical domain of the influenza virus NS1 protein requires its dimer structure and a small number of specific basic amino acids. *RNA* **5,** 195–205.

Zorn, A. M., and Krieg, P. A. (1997). The KH domain protein encoded by quaking functions as a dimer and is essential for notochord development in Xenopus embryos. *Genes Dev.* **11,** 2176–2190.

Received for publication August 6, 2001
Revised March 28, 2002
Accepted March 28, 2002
Published online May 24, 2002